RSC Advances

ROYAL SOCIETY OF CHEMISTRY

www.rsc.org/advances

Journal Name

RSCPublishing

COMMUNICATION

Nitrogen Doped Graphene Paper as Highly Conductive, and Light-weight Substrate for Flexible Supercapacitors

Cite this: DOI: 10.1039/x0xx00000x

Received 00th January 2012,
Accepted 00th January 2012

DOI: 10.1039/x0xx00000x

www.rsc.org/

Cheng Li, [a] Yue Hu, [a] Minghao Yu, [a] Wenxia Zhao,[b] Peng Liu, [a]* Yexiang Tong, [a] and Xihong Lu[a]*

In this work, we fabricated a lightweight (1.25 g cm^{-3}) N doped reduced graphene (N-RGO) paper through a combination method of vacuum filtration method and thermal treatment under ammonia atmosphere. 0.48% of N element has been uniformly incorporated into the graphene sheets, which results in an inherently improvement in conductivity. Simultaneously, the as-fabricated N-RGO paper possesses excellent flexibility without any effect on its electronic property. Furthermore, the good performance of N-RGO as supercapacitor electrode was also demonstrated with a high specific capacitance of 280 F g^{-1} at 5 mV s^{-1}. N-RGO electrode also exhibited a remarkable long-term cycling stability with 99.4% capacitance retention after 40000 cycles. This work constitutes the first attempt of applying N-doping to improve the electronic property and electrochemical performance for graphene paper.

Graphene, as a monolayer of sp^2 bonded carbon combining superior electronic conductivity, high mechanical flexibility, and high specific surface, has attracted tremendous attention in a broader range of application[1-6]. Motivated by the strong demand of its convenient application in transistors[7], solar cells[8], sensors[9], energy storage[10] and biochemical fields[11], several research attempts focused on integrating individual graphene sheets into macroscopic structures like graphene foams[12-14], graphene aerogels[15, 16], graphene sponges[17, 18] *etc.* Apart from these, Ruffo and his co-workers creatively assembled a novel free-standing graphene oxide (GO) paper through filtration of dispersed GO aqueous solution.[19] Immediately following, Li *et al.* adopted this technique to prepare graphene paper by a further reduction step.[20] Such fabricated graphene paper possesses very high mechanical stiffness, excellent flexibility and ultralight weight without additives or current collectors, which particularly suit for fabricating flexible energy storage electrode. For instance, Li and his group explored the electrochemical performance of such paper as supercapacitor electrode.[21] A maximum specific capacitance of 70 F g^{-1} at 100 A g^{-1} was achieved with a mass density of 0.45 mg cm^{-2}. However, the capacity of graphene paper only derived from double layer capacitance is still unsatisfactory and far from meeting the requirement of practical application. Hence, it is still highly desired to improve its specific capacitance.

To inherently improve the electronic characteristic of graphene materials, one effective strategy is chemical doping with foreign atoms into them. Among the numerous potential dopants, nitrogen has been widely employed to enrich free charge-carrier density and improve the electrical conductivity of graphene materials.[22-33] That can be attributed to its comparable atomic size with carbon atoms and five valence electrons which are able to form strong valence bonds with carbon. To date, extensive efforts have been devoted to studying the promising application of nitrogen doped graphene materials like water splitting[28, 29], fuel cell[22], sensor[24, 31], lithium battery[23, 32] and supercapacitors[26, 27]. However, reports on the application of nitrogen-doped graphene in supercapacitors are still scarce. And to our knowledge, there is still few attempts that applying nitrogen-doping to modify the electronic and electrochemical properties of graphene paper. Hence, a huge capacitive enhancement is expected for graphene paper based electrodes through such modification.

With this motivation, we developed reduced graphene oxide (RGO) paper via vacuum filtration of aqueous graphene oxide (GO) dispersion and a chemical reduction process. Nitrogen doping was followed through a thermal treatment under ammonia atmosphere. Uniformly incorporation of N element into graphene sheet was confirmed by EELS elemental mapping and XPS results. The amount of N is only 0.48% with a form of pyridine-like N. As a result, the conductivity of N-doping reduced graphene oxide (N-RGO) paper got a substantially increase. Furthermore, the excellent mechanical property of the as-fabricated N-RGO paper was confirmed without sacrifice of its electronic property, which enables its promising application in flexible electronics. Hence, we tested the

performance of N-RGO as supercapacitor electrode. A high specific capacitance of 280 F g^{-1} at 5 mV s^{-1}, which is considerably higher than that of RGO electrode (29 F g^{-1}). And a perfect stability was also obtained with almost no decrease of specific capacitance after 40000 cycles at 100 mV s^{-1}. We believe that such good electrochemical performance pave the way for facilitating the fabrication of flexible graphene-based electronic devices for a broader range of application.

Experimental methods

Preparation of graphene oxide aqueous solution

Graphene oxide was prepared by oxidizing natural graphite powder, according to a modified Hummers method. Briefly, graphite powder (1 g) was added to a mixture of concentrated H_2SO_4 (40 mL) and concentrated HNO_3(10 mL) that was cooled in an ice bath. $KMnO_4$ was then slowly added to the solution and maintained for 2h at 35 ^oC, followed by dilution using deionized water (280 mL). After that a H_2O_2 solution was added to the mixture until gas bubbles no longer evolved, accompanied by gradually converting into a bright yellow solution. The solid graphene obtained from centrifugation was washed with 15 vol% HCl and deionized water, and each washing process was repeated for three times. Finally, the Graphene oxide was dissolved into 0.4 mg mL^{-1} aqueous solution.

Preparation of N-RGO paper

GO paper, the precursor of RGO paper, was prepared by vacuum filtration of the as-prepared graphene oxide aqueous solution through an Anodisc membrane filter (47 mm in diameter, 0.2 μm pore size, Millipore membranes), followed by air drying and peeling from the filter. Then, GO paper was reduced into RGO paper by hydrazine vapor. In details, GO paper was placed in a sealed container, which contained 2 mL of hydrazine. Then the container was heated at 85 ^oC for 24 h. Finally, N-RGO paper was obtained by annealing at 800 ^oC in ammonia for 1h.

Fabrication of N-RGO based solid state supercapacitors

PVA (2 g) was dissolved in 20 mL of 1M H_2SO_4 solution at 85 °C, until they completely dissolved in water and formed a jelly-like solution. Two pieces of N-RGO electrodes with a working area of 0.5 cm^2 and a piece of filter paper were soaked in the gel electrolyte for 1 min to allow the electrolyte to diffuse into the nanoporous structure of N-RGO electrode; they were then removed and allowed them to dry under ambient conditions for 10 min. This gel coating process was repeated three times. The symmetrical SSC device was fabricated by sandwiching the filter paper (serving as a separator) with two pieces of N-RGO electrodes.

Material Characterization and Electrochemical Measurement

The microstructures and compositions of electrode materials were analyzed by field-emission SEM (FE-SEM, JSM-6330F), Raman spectroscopy (Renishaw inVia), transmission electron microscopy (TEM, FEI Tecnai G^2 F30), XPS (XPS, ESCALab250, Thermo VG) and Fourier transform infrared spectroscopy (FTIR, Bruker, EQUINOX 55). The surface area of the product was calculated from nitrogen adsorption/desorption isotherms at 77 K that were conducted on an ASAP 2020 V3.03 H instrument. Prior to measurement, all samples were outgassed at 100 ^oC for 300 min under flowing nitrogen. The conductivity of products was measured by a standard four-probe method using a physical property measurement system (ST2253). Cyclic voltammetry (CV), galvanostatic charge/discharge measurements and electrochemical impedance electrochemical workstation (CHI 760E). The electrochemical studies of RGO (0.5×1 cm^2) and N-RGO electrodes (0.5×1 cm^2) were performed in a conventional three-electrode cell, using a Pt counter electrode and a Ag/AgCl reference electrode with 1 M H_2SO_4 electrolyte.

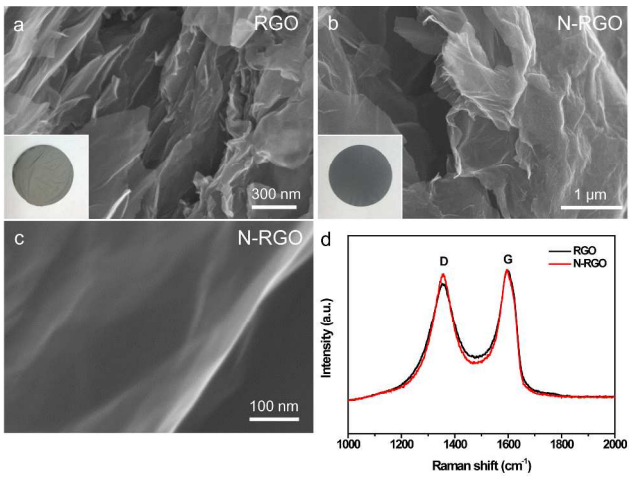

Figure 1. (a) and (b) SEM images and digital pictures (insets) of RGO paper and N-RGO paper. (c) Magnified SEM image of N-RGO paper. (d) Raman spectra of RGO paper and N-RGO paper.

In the present work, a colloidal suspension of GO with a concentration of 0.4 mg mL^{-1} was utilized to fabricate GO paper by vacuum filtration. Then the GO paper was reduced into RGO paper using hydrazine hydrate vapor. The as-fabricated macroscopic RGO paper is very light-weight (about 1.25 g cm^{-3}) and dark brown with a few centimeters in size (inset of Figure 1a). Scanning electron microscopy (SEM) image in Figure 1a reveals that the partial overlapping or coalescence of thin RGO sheets resulted in an interconnected three-dimensional (3D) porous structure of this RGO paper. The pore size of the network ranged about hundreds of nanometers to several micrometers, which could provide effective diffusion channels for ion transport in the electrolyte. Nitrogen was introduced into the RGO paper by a simple thermal treatment at 800 ^oC under ammonia atmosphere. Figure 2b and Figure S1 displays the SEM image of as-fabricated N-RGO paper, from which it can be concluded that the macrostructure is well preserved during the thermal treatment process. The thickness was acquired to be about 20 μm from Figure S1. The N_2 absorption Brunauer-Emmett-Teller (BET) measurement of our N-RGO paper also reveals a high surface area of 298 m^2 g^{-1}. Meanwhile, the color of N-RGO paper changed into dark blue. Ripples and winkles caused by the high surface energy of graphene sheets was demonstrated by its magnified SEM image in Figure 2c, leading to much higher surface area. Furthermore, Raman spectra were collected for RGO and N-RGO paper as presented in Figure 2d. Two typical peaks located at 1357 cm^{-1} and 1593 cm^{-1} respectively respond to the D-band and G-band of graphene[23, 25, 34, 35]. The intensity ratio of these two peaks, which is denoted as I_D/I_G, provides the information of structural defects and edge plane exposure. As can be observed, the I_D/I_G shows a slight increase from 0.89:1 to 0.97:1 after the thermal treatment process, indicating the enriched presence of defects in N-RGO paper. These defects are attributed to the heterogeneous nitrogen atom incorporation into the graphene layers.[25]

The direct evidence for N-doping in N-RGO was obtained by transmission electron microscope (TEM) image and electron energy-loss spectroscopy (EELS) in Figure 2. Figure 2a presents the typical TEM image of N-RGO, of which the low contrast image indicates only a few layers of graphite sheets constructs the graphene layer. EELS spectrum of the circle area in Figure 2a was acquired at an energy range containing the C-K edge and the N-K edge, with an energy resolution of 1.0 eV, which is shown in Figure 2b. The peak located at 285 eV corresponds to excitation of the 1s carbon electrons toward the π* states, while the peak at 291 eV is attributed

to excitation from the 1s to the σ* states.[36] These two peaks are the main features of a graphite EELS in the carbon K-edge region. The weak features at around 401 eV attributed to nitrogen K-edge region is due to the trace amount of nitrogen.[37] From the quantitative EELS analysis, the atomic ratio of C to N is calculated to be 99.52:0.48. Besides, the uniform distribution of nitrogen along with carbon over the whole graphene sheet was confirmed by the EELS elemental mapping as presented in Figure 2c and 2d.

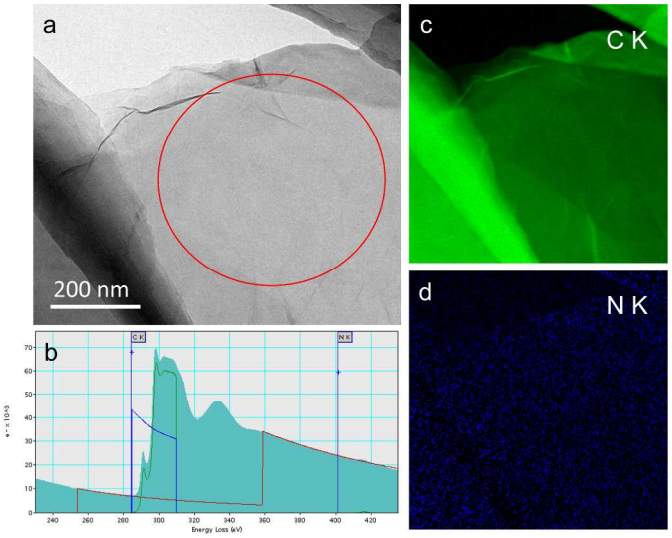

Figure 2. (a) Typical TEM image of N-RGO paper. (b). An EELs spectrum image was acquired from the squared area in (a). EELS mapping images of (c) carbon and (d) nitrogen.

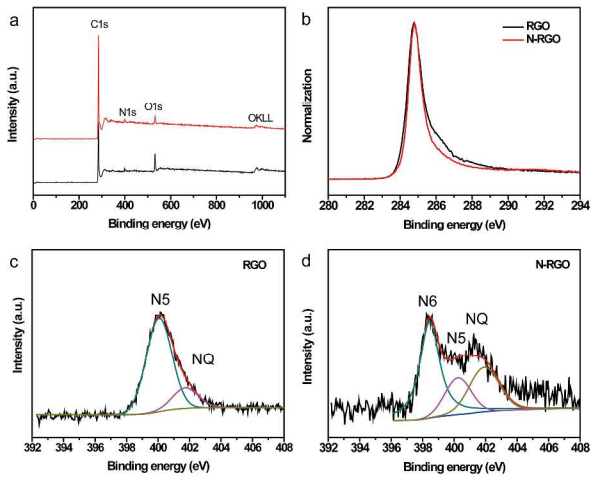

Figure 3. (a) XPS survey spectrum and (b) corresponding high-resolution C1s peak of RGO paper and N-RGO paper. (c) High-resolution N1s peak of RGO paper. (d) High-resolution N1s peak of N-RGO paper.

The nature of the binding between carbon and nitrogen was further probed through X-ray photoelectron spectroscopic (XPS) measurements. As can be seen from Figure 3a, both RGO paper and N-RGO paper contain a dominant C1s peak, a weak O1s peak and a recognizable N1s peak with no evidence of impurity. In particular is that traces of nitrogen element were introduced during hydrazine reduction process. Figure 3b compares the high resolution C1s spectra for RGO and N-RGO. The obvious subdued peak around 286.5 eV proved that residual oxygen-containing groups were further removed upon thermal annealing in ammonia atmosphere. Furthermore, high resolution N1s spectra were analyzed for both RGO and N-RGO (Figure 3c and 3d). The N1s peak for RGO can be resolved into two peaks located at 400.0 and 401.7 eV representing pyrrole-like N (denoted as N5) and graphitic N (denoted as NQ).[24, 38] Meanwhile, in addition to these two peaks, a peak at 401.7 eV was acquired in N1s peak for N-RGO, which takes account for the pyridine-like N (denoted as N6).[24, 38] Besides, an additional absorption of Fourier transform infrared spectroscopy (FTIR) around 1580 cm^{-1} appeared for N-RGO paper, which is associated with the newly formed C=N bonding (Figure S2). All these results revealed that N atoms have been incorporated into the carbon–carbon bonds of graphene for N-RGO. The extra introduction of pyridine-like N is expected to inherently tune the electronic property of graphene and serve as additional active sites for capacitive behavior.

As two essential parameters for flexible electronic application, conductivity and mechanical property were further evaluated for the as-fabricated N-RGO paper. Linear sweep voltammograms (LSV) curves collected for RGO and N-RGO were displayed in Figure 4a. In comparison to the curve of RGO paper, the much higher slope obtained for that of N-RGO paper suggests its superior conductivity. Simultaneously, the conductivity of N-RGO paper was measured by a standard four-probe method. The calculated conductivity is 316 S cm^{-1}, which is considerably higher than our RGO paper (52 S cm^{-1}) and recently reported RGO paper[10, 39-41]. That can be attributed to that doped nitrogen plays a critical role in regulating the electronic properties of graphene even though the amount is small. In order to highlight the stable mechanical property of N-RGO, its conductive variation was studied under both static and dynamic bending conditions. As shown in Figure 4b, no obvious change was observed for the conductivity when N-RGO paper under different bend condition. Simultaneously, N-RGO retained 99.7 % of its initial conductivity after 500 bending cycles (Figure 4c), which means the folding of N-RGO do not affect its electronic property. Furthermore, the as-fabricated N-RGO paper could also sustain a certain of mechanical strain as shown in Figure 4d. The change of electrical resistance is negligible for N-RGO paper even the strain up to 1 %. Overall, all these unique properties enable our N-RGO paper to be directly used as electrode or serve as excellent conductive substrate for flexible electronic applications.

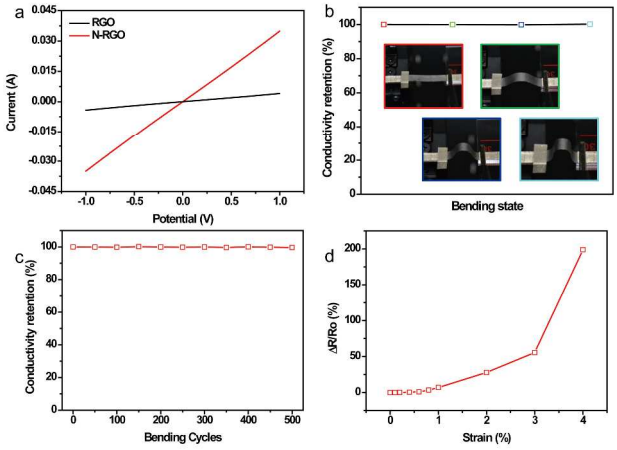

Figure 4. (a) Linear sweep voltammograms curves for RGO paper and N-RGO paper. (b) Conductivity retention of N-RGO paper under different bending condition. (c) Conductivity retention of N-RGO paper as a function of bending cycle number. (d) Resistance variation of N-RGO paper under different strain.

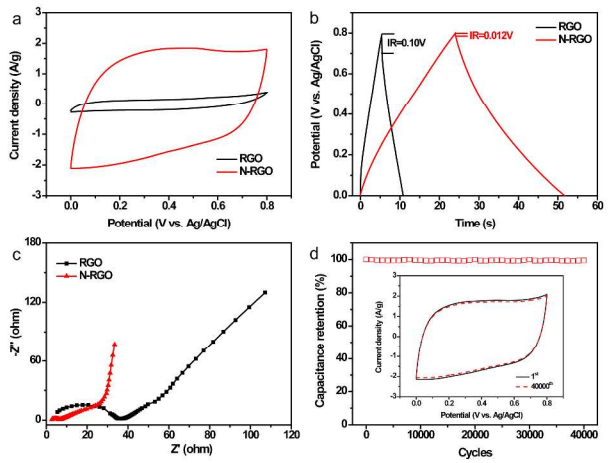

Figure 5. (a) CV curves of RGO and N-RGO electrodes collected at a scan rate of 5 mV s^{-1}. (b) Single cycle of galvanostatic curves collected at a current density of 5 A g^{-1} for RGO and N-RGO electrodes. (c) Nyquist plots for RGO and N-RGO electrodes. (d) Cycling performance of N-RGO electrode collected at 100 mVs^{-1}. Insets: CV curves collected at 100 mV s^{-1} of N-RGO electrode before and after testing for 40000 cycles.

Consequently, the influence of N-doping on the electrochemical performance of graphene paper was evaluated. All electrochemical measurements were conducted in a simple three-electrode cell in a 1 M H_2SO_4 aqueous electrolyte, with a Pt counter electrode and an Ag/AgCl reference electrode. Figure 5a compares the cyclic voltammogram (CV) curves of RGO and N-RGO electrode at a scan rate of 5 mV s^{-1}. Both curves present symmetric and approximately rectangle-like shape, suggesting their ideal capacitive behavior. As expected, considerably enhanced current density of the CV curve by more than one order of magnitude was reached by N-RGO electrode in comparison with RGO electrode. The calculated specific capacitance for N-RGO electrode achieves 280 F g^{-1}, which is not only much higher than that of RGO electrode (only 29 F g^{-1}), but also substantially higher than recently reported graphene based electrodes like folded structured graphene paper (172 F g^{-1} at 1 A g^{-1}),[41] graphene hydrogel (187 F g^{-1} at 1 A g^{-1}),[42] graphene aerogel (128 F g^{-1} at 0.05 A g^{-1})[16] and nitrogen doped graphene aerogel (175 F g^{-1} at 5 mV s^{-1})[38]. The CV curves of N-RGO electrode collected at different scan rates are shown in Figure S3. All the curves show essentially similar and symmetric shape as the scan rate increases from 5 to 200 mV s^{-1}, indicating the good capacitive behavior of N-RGO electrode. Significantly, N-RGO electrode expressed a good rate capability with a retention of 33% of the initial capacitance when the scan rate was increased 40-fold from 5 to 200 mV s^{-1}. This efficient electrical double layer formation can be attributed to the unique porous structure and superior conductivity of N-RGO electrode. Galvanostatic charge/discharge curves of RGO and N-RGO electrodes collected at 5 A g^{-1} are shown in Figure 5b. Consistent with CV results, the substantially longer discharge time of N-RGO electrode again confirms its superior capacitive behavior. Additionally, the IR drop of N-RGO electrode is much smaller than that of RGO electrode, implying the conductivity was significantly improved after introducing pyridine-like N. Electrochemical impedance spectroscopy (EIS) measurement was also conducted to better understand these electrodes. Figure 5c compares the Nyquist plots of RGO and N-RGO electrodes. It is derived that N-RGO electrode owns lower charge-transfer resistance and faster diffusion of ions in electrolyte from its smaller diameter of the semicircle in the high-medium frequency and more steeper straight line in low frequency region. Thereby, the main reason for the much superior capacitive behavior of N-RGO can be attributed to the inherently improved conductivity and extra introduced capacitance caused by the doped pyridine-like N, even though the amount is only 0.48 %. The long-term cycling performance of the N-RGO electrode was tested at 100 mV s^{-1}. The N-RGO electrode possessed a ultrahigh electrochemical stability of 99.4% capacitance retention after 40000 cycles (Figure 5d), which is also an excellent result among graphene based electrodes.[16, 38, 41-43] The CV curves of N-RGO electrode at 100 mV s^{-1} before and after cyclic testing almost have no difference.

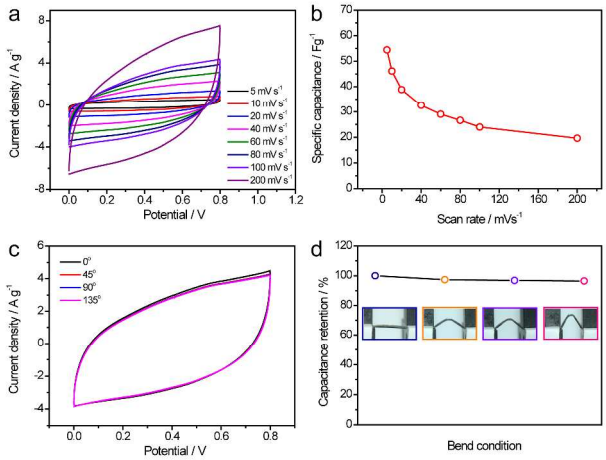

Figure 5. (a) CV curves of the as-fabricated N-RGO-SSC device collected at different scan rate. (b) Specific capacitance of the SSC device calculated from the CV curves as a function of scan rate. (c) CV curves collected at a scan rate of 100 mV s^{-1} for the SSC device under different bending conditions. (d) Capacitance retention of the SSC device under different bending conditions. Insets are the device picture under test conditions.

Finally, to test the feasibility of N-RGO paper as electrode for flexible supercapacitors, a solid state flexible device (N-RGO-SSC) was fabricated by using two identical N-RGO electrodes with H_2SO_4/PVA electrolyte and a separator (Figure 5). The device achieved an excellent specific capacitance of 54.5 F g^{-1} at 5 mV s^{-1}. which is substantially higher than recently reported carbon material based symmetric supercapacitors[34, 44-47]. Moreover, the CV curves collected for the device under different bend conditions are almost the same (Figure 5c, d), and the variation of calculated specific capacitance is less than 4%. All these results confirmed that our N-RGO electrode can be applied into fabricating flexible supercapacitors.

Conclusion

In summary, we fabricated a kind of RGO paper through a vacuum filtration method. N element was further introduced into this paper using thermal treatment under ammonia atmosphere. EELs elemental mapping and XPS confirmed that the N element has uniformly incorporated into graphene sheet as a form of pyridine-like N. Although the amount of N is only 0.48%, the conductivity of as-fabricated N-RGO paper got inherently improved. Simultaneously, the excellent mechanical property of N-RGO was also demonstrated. Considering all these good properties, N-RGO paper has great promising in

flexible electronic device. As a demonstrated, its electrochemical performance as supercapacitor electrode was further evaluated. N-RGO electrode exhibited a much superior capacitive behavior to RGO electrode. A high specific capacitance of 280 F g^{-1} at 5 mV s^{-1} was achieved, and a good long-term cycling stability with almost no decrease in capacitance after 40000 cycles was also acquired. Given the remarkable electrochemical performance, we believe the current work will open new possibilities in flexible energy storage.

Acknowledgements

We acknowledge the financial support by the Natural Science Foundations of China (21273290, 91323101, and J1103305), the Natural Science Foundations of Guangdong Province (S2013030013474), and the Research Fund for the Doctoral Program of Higher Education of China (20120171110043).

Notes and references

[a] MOE of the Key Laboratory of Bioinorganic and Synthetic Chemistry, KLGHEI of Environment and Energy Chemistry, School of Chemistry and Chemical Engineering, Sun Yat-Sen University, Guangzhou 510275, People's Republic of China. Email: luxh6@mail.sysu.edu.cn (X. H. Lu); ceslp@mail.sysu.edu.cn (P. Liu).
[b] Instrumental Analysis & Research Center, Sun Yat-Sen UniVersity, Guangzhou 510275, China

Electronic Supplementary Information (ESI) available: Detailed experimental section. See DOI: 10.1039/c000000x/

1 K. S. Novoselov, A. K. Geim, S. V. Morozov, D. Jiang, Y. Zhang, S. V. Dubonos, I. V. Grigorieva and A. A. Firsov, *Science*, 2004, **306**, 666-669.
2 Y. Kopelevich and P. Esquinazi, *Adv. Mater.*, 2007, **19**, 4559-4563.
3 A. K. Geim and K. S. Novoselov, *Nat. Mater.*, 2007, **6**, 183-191.
4 X. Liu, M. Zheng, K. Xiao, Y. Xiao, C. He, H. Dong, B. Lei and Y. Liu, *Nanoscale*, 2014, **6**, 4598-4603.
5 B. Li, Y. Cheng, J. Liu, C. Yi, A. S. Brown, H. Yuan, T. Vo-Dinh, M. C. Fischer and W. S. Warren, *Nano Lett.*, 2012, **12**, 5936-5940.
6 L. Shao, X. Wang, H. Xu, J. Wang, J.-B. Xu, L.-M. Peng and H.-Q. Lin, *Adv.Opt.Mater*, 2014, **2**, 162-170.
7 Y. M. Lin, C. Dimitrakopoulos, K. A. Jenkins, D. B. Farmer, H. Y. Chiu, A. Grill and P. Avouris, *Science*, 2010, **327**, 662.
8 J. Liu, Y. Xue, Y. Gao, D. Yu, M. Durstock and L. Dai, *Adv. Mater.*, 2012, **24**, 2228-2233.
9 F. Schedin, A. K. Geim, S. V. Morozov, E. W. Hill, P. Blake, M. I. Katsnelson and K. S. Novoselov, *Nat. Mater.*, 2007, **6**, 652-655.
10 X. Zhao, C. M. Hayner, M. C. Kung and H. H. Kung, *ACS Nano*, 2011, **5**, 8739-8749.
11 W. Hu, C. Peng, W. Luo, M. Lv, X. Li, D. Li, Q. Huang and C. Fan, *ACS Nano*, 2010, **4**, 4317-4323.
12 Z. Chen, W. Ren, L. Gao, B. Liu, S. Pei and H. M. Cheng, *Nat. Mater.*, 2011, **10**, 424-428.
13 T. Zhai, F. Wang, M. Yu, S. Xie, C. Liang, C. Li, F. Xiao, R. Tang, Q. Wu, X. Lu and Y. Tong, *Nanoscale*, 2013, **5**, 6790-6796.
14 Z. Niu, L. Liu, L. Zhang and X. Chen, *Small*, 2014, DOI: 10.1002/smll.201400128.
15 Y. Xu, K. Sheng, C. Li and G. Shi, *ACS Nano*, 2010, **4**, 4324-4330.
16 X. Zhang, Z. Sui, B. Xu, S. Yue, Y. Luo, W. Zhan and B. Liu, *J. Mater. Chem.*, 2011, **21**, 6494.
17 H. B. Yao, J. Ge, C. F. Wang, X. Wang, W. Hu, Z. J. Zheng, Y. Ni and S. H. Yu, *Adv. Mater.*, 2013, **25**, 6692-6698.
18 H.-W. Liang, Q.-F. Guan, Z. Zhu, L.-T. Song, H.-B. Yao, X. Lei and S.-H. Yu, *NPG Asia Mater.*, 2012, **4**, e19.
19 D. A. Dikin, S. Stankovich, E. J. Zimney, R. D. Piner, G. H. Dommett, G. Evmenenko, S. T. Nguyen and R. S. Ruoff, *Nature*, 2007, **448**, 457-460.
20 H. Chen, M. B. Müller, K. J. Gilmore, G. G. Wallace and D. Li, *Adv. Mater.*, 2008, **20**, 3557-3561.
21 X. Yang, J. Zhu, L. Qiu and D. Li, *Adv. Mater.*, 2011, **23**, 2833-2838.
22 L. Qu, Y. Liu, J. B. Baek and L. Dai, *ACS Nano*, 2010, **4**, 1321-1326.
23 A. L. Reddy, A. Srivastava, S. R. Gowda, H. Gullapalli, M. Dubey and P. M. Ajayan, *ACS Nano*, 2010, **4**, 6337-6342.
24 Y. Wang, Y. Shao, D. W. Matson, J. Li and Y. Lin, *ACS Nano*, 2010, **4**, 1790-1798.
25 D. Geng, Y. Chen, Y. Chen, Y. Li, R. Li, X. Sun, S. Ye and S. Knights, *Energy Environ. Sci.*, 2011, **4**, 760.
26 H. M. Jeong, J. W. Lee, W. H. Shin, Y. J. Choi, H. J. Shin, J. K. Kang and J. W. Choi, *Nano Lett.*, 2011, **11**, 2472-2477.
27 Y. Zhao, C. Hu, Y. Hu, H. Cheng, G. Shi and L. Qu, *Angew. Chem. Int. Ed.*, 2012, **124**, 11533-11537.
28 S. Chen, J. Duan, J. Ran, M. Jaroniec and S. Z. Qiao, *Energy Environ. Sci.*, 2013, **6**, 3693.
29 S. Chen and S. Z. Qiao, *ACS Nano*, 2013, **7**, 10190-10196.
30 M. Fan, C. Zhu, Z. Q. Feng, J. Yang, L. Liu and D. Sun, *Nanoscale*, 2014, **6**, 4882-4888.
31 Z. Juanjuan, L. Ruiyi, L. Zaijun, L. Junkang, G. Zhiguo and W. Guangli, *Nanoscale*, 2014, **6**, 5458-5466.
32 L. L. Tian, X. Y. Wei, Q. C. Zhuang, C. H. Jiang, C. Wu, G. Y. Ma, X. Zhao, Z. M. Zong and S. G. Sun, *Nanoscale*, 2014, **6**, 6075-6083.
33 L. Liu, Z. Niu, L. Zhang and X. Chen, *Small*, 2014, **10**, 2200-2214.
34 G. Wang, H. Wang, X. Lu, Y. Ling, M. Yu, T. Zhai, Y. Tong and Y. Li, *Adv. Mater.*, 2014, **26**, 2676-2682.
35 L. Liu, Z. Niu, L. Zhang, W. Zhou, X. Chen and S. Xie, *Adv. Mater.*, 2014, DOI: 10.1002/adma.201401513.
36 M. H. Gass, U. Bangert, A. L. Bleloch, P. Wang, R. R. Nair and A. K. Geim, *Nat. Nanotechnol.*, 2008, **3**, 676-681.
37 L. S. Zhang, X. Q. Liang, W. G. Song and Z. Y. Wu, *Phys. Chem. Chem. Phys.*, 2010, **12**, 12055-12059.
38 Z. S. Wu, A. Winter, L. Chen, Y. Sun, A. Turchanin, X. Feng and K. Mullen, *Adv. Mater.*, 2012, **24**, 5130-5135.
39 L. Qiu, J. Z. Liu, S. L. Chang, Y. Wu and D. Li, *Nat. Commun.*, 2012, **3**, 1241.
40 H. Gwon, H.-S. Kim, K. U. Lee, D.-H. Seo, Y. C. Park, Y.-S. Lee, B. T. Ahn and K. Kang, *Energy Environ. Sci.*, 2011, **4**, 1277.
41 F. Liu, S. Song, D. Xue and H. Zhang, *Adv. Mater.*, 2012, **24**, 1089-1094.
42 L. Zhang and G. Shi, *J. Phys. Chem. C* 2011, **115**, 17206-17212.
43 G. Wang, X. Sun, F. Lu, H. Sun, M. Yu, W. Jiang, C. Liu and J. Lian, *Small*, 2012, **8**, 452-459.
44 S. Hu, R. Rajamani and X. Yu, *Appl. Phys. Lett.*, 2012, **100**, 104103.
45 C. Du, J. Yeh and N. Pan, *Nanotechnology*, 2005, **16**, 350-353.
46 M. Kaempgen, C. K. Chan, J. Ma, Y. Cui and G. Gruner, *Nano Lett.*, 2009, **9**, 1872-1876.
47 D. N. Futaba, K. Hata, T. Yamada, T. Hiraoka, Y. Hayamizu, Y. Kakudate, O. Tanaike, H. Hatori, M. Yumura and S. Iijima, *Nat. Mater.*, 2006, **5**, 987-994.

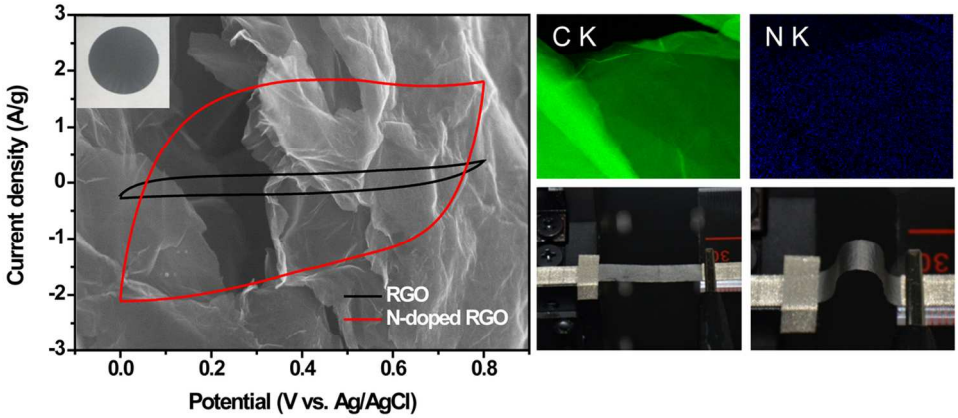

118x55mm (300 x 300 DPI)